



Article

Isotopic Composition of Spring Water in Greece: Spring Waters Isoscapes

Dotsika Elissavet ^{1,*} , Diamantopoulos George ¹, Lykoudis Spyridon ² , Poutoukis Dimitrios ³ and Kranioti Elena ⁴

¹ National Center of Scientific Research “Demokritos”, Institute of Materials Science, GR15310 Ag. Paraskevi Attikis, Greece; g.diamantopoulos@inn.demokritos.gr

² Independent Researcher, Akrita 66, gr 24100 Kalamata, Greece; slykoud@yahoo.com

³ General Secretariat for research and Technology, Mesogion 14-18, 11510 Athens, Greece; dpoutoukis@gsrt.gr

⁴ Edinburgh Unit for Forensic Anthropology, School of History, Classics and Archaeology, William Robertson Wing, University of Edinburgh, Old Medical Quad, Teviot Place, Edinburgh EH8 9AG, UK; Elena.Kranioti@ed.ac.uk

* Correspondence: e.dotsika@inn.demokritos.gr; Tel. +30-2106503305

Received: 21 May 2018; Accepted: 25 June 2018; Published: 28 June 2018



Abstract: This paper reviews stable isotopic data concerning spring water in Greece in addition to new measurements (59); their spatial variations are investigated in order to provide basic information and identify the locally significant parameters that affect stable isotopic distributions. The area of interest was partitioned into eight sections according to geographical location and climatic characteristics. Local spring water lines (LSWLs) are more or less consistent throughout the country. High-resolution isoscape maps of spring freshwater ($\text{Cl}^- < 200$ ppm; and $T < 25$ °C) for both $\delta^{18}\text{O}$ and $\delta^2\text{H}$ were generated, revealing several interesting features such as the effect of Pindos ridge, a strong climatic signal in southern Greece and indications of seawater intrusion in flat coastal areas.

Keywords: spring water; stable isotopes; isoscapes; gridded data

1. Introduction

The isotopic composition of spring water in Greece is mainly affected by: its location within the Mediterranean basin (the eastern Mediterranean basin is dominated by air masses on the leeside of the continental areas due to intense evaporation of seawater in conditions of moisture deficit [1,2]); a complex morphology dominated by the presence of the Pindos ridge range crossing Greece from NW to SE (and practically acting as a barrier to the precipitation); and the existence of the Ionian and Aegean seas around Greece (that further affect the precipitation patterns).

Finally, the lack of a dense sampling network that would be representative of all altitudes and sides of Greece further complicates the situation.

The use of stable isotopic analyses for investigating paleodiet [3,4], and paleoclimate has generally proceeded on two fronts: evaluation of the stable isotope compositions in various natural systems to understand the biological and geological processes, and subsequently to generate predictive models. These models incorporate spatially variable isotopic parameters to construct isotope “iso-land-scapes” and have been previously used to trace the origin of unknown ecological (plants, natural products, animals, humans) and geological (soil, minerals, water) samples.

The use of isotope analysis in modern forensic work would not be possible without the pioneering work in the fields of geology, hydrogeology, anthropology, archaeology, ecology, and plant physiology. In particular, the oxygen and hydrogen isotope analysis of water led to the construction of the first *isoscape* maps, setting the foundation for isotope forensics studies. This isoscape approach has provided

an empirical framework from which it is possible to predict the geographic origin of unknown samples and even identify the residence patterns of unidentified human remains based on their isotopic signatures (bone, teeth, hair, and nails) [5–9].

In this study, we present the oxygen and deuterium isotope composition of spring waters from Greece aiming to evaluate the spatial variability of spring water composition and its possible relation to the isotopic composition of precipitation. We present high-resolution isoscape maps of the spatial distribution of spring water $\delta^{18}\text{O}$ – $\delta^2\text{H}$ that could provide important information for hydrological studies and represent a reference for the assessment of future changes. These maps are the result of on-going research and are being constantly improved (with new samples and different sampling years). The same isoscape maps can be used in archaeological studies, like those focused on paleodiet and paleoclimate, as well as in contemporary forensic studies. Furthermore, we present the Cl^- composition of the spring waters (including springs with high Cl^- concentrations) and evaluate the mixing ratio with seawater.

2. Data and Methods

An extensive literature review was performed in order to gather all available data on the isotopic composition of water in Greece. Spring water and seawater isotopic, chemical, and physical data were compiled from international and Greek sources [10–39].

In this work only data from springs were considered, corresponding to $\text{Cl}^- \leq 200$ ppm and $T \leq 25$ °C, if those parameters were available. For those springs with more than one record, mean values were calculated, resulting in 369 (suppl. information of ref. [40]) records for $\delta^{18}\text{O}$ and $\delta^2\text{H}$. In addition, some 74 unpublished measurements (Table 1) made by the authors according to the procedures described by Epstein [41] and Coleman [42] by means of Finnigan Delta V Plus mass spectrometers were also included, bringing the total up to 443. The geographical distribution of the stations considered in this work is presented in Figure 1.

Table 1. General isotopic ($\delta^{18}\text{O}$ and $\delta^2\text{H}$) values of 74 Greek spring waters.

NO	Spring	Location	Region	North	East	Sampling Date	$\delta^{18}\text{O}$ (‰, VSMOW)	$\delta^2\text{H}$ (‰, VSMOW)
1	Chaladra	Chios	Aegean Isl.	38.55	25.94	2018	−7.2	−43.5
2	Nagos	Chios	Aegean Isl.	38.56	26.07	2018	−7.3	−45.1
3	Ag. Fokas1	Kos	Aegean Isl.	36.85	27.25	2018	−6.3	−38.1
4	Ag. Fokas2	Kos	Aegean Isl.	36.86	27.26	2018	−6.0	−31.1
5	Makriammos	Thasos	Aegean Isl.	40.76	24.73	2018	−8.1	−50.1
6	Potamia	Thasos	Aegean Isl.	40.71	24.72	2018	−8.1	−49.4
7	Therisso	Chania	Crete	35.24	23.59	2014	−8.8	−52.5
8	Sterna	Heraklion	Crete	35.01	25.08	2014	−7.7	−53.1
9	Foteino	Arta	Epirus	39.09	21.04	2016	−5.8	−35.1
10	Graikiko	Ioannina	Epirus	39.42	21.04	2016	−7.1	−41.5
11	Kranoula	Ioannina	Epirus	39.55	29.45	2015	−8.3	−52.5
12	Kranoula	Ioannina	Epirus	39.55	29.45	2016	−8.1	−51.5
13	Mili	Ioannina	Epirus	39.78	21.1	2016	−7.3	−43.9
14	Sepeta (s)	Ioannina	Epirus	38.45	20.5	2015	−8.3	−52.3
15	Sepeta (s)	Ioannina	Epirus	39.45	20.5	2016	−7.7	−50.5
16	Vathipedo	Ioannina	Epirus	39.62	21.08	2016	−8.1	−52.6
17	Vikos	Ioannina	Epirus	39.57	20.42	2015	−8.0	−54.9
18	Vikos	Ioannina	Epirus	39.57	20.42	2016	−7.7	−52.6
19	Nea Tenedos	Chalkidiki	Macedonia	40.32	23.25	2014	−6.8	−46.9
20	Petralona	Chalkidiki	Macedonia	40.37	23.17	2014	−8.6	−62.1
21	Polygiros	Chalkidiki	Macedonia	40.23	23.27	2018	−8.2	−51.5
22	Kato Nevrokopi	Drama	Macedonia	40.88	24.09	2016	−8.2	−54.1
23	Anthemia	Imathia	Macedonia	40.28	23.02	2014	−7.6	−49.3
24	Anthemia	Imathia	Macedonia	40.28	23.02	2018	−7.7	−50.3
25	Korifes	Kavala	Macedonia	41.06	24.45	2014	−8.0	−47.0
26	Makrinita	Kilkis	Macedonia	41.3	22.99	2016	−7.2	−45.3
27	Notia	Kilkis	Macedonia	41.06	22.07	2016	−9.3	−64.5
28	Kopanou	Kozani	Macedonia	40.64	22.12	2014	−9.3	−65.2
29	Drosia	Pella	Macedonia	40.47	21.52	2016	−9.1	−62.8
30	Polichni	Thessaloniki	Macedonia	40.67	22.96	2014	−7.1	−44.9
31	Vlacherna	Arkadia	Peloponnese	37.71	22.23	2015	−7.9	−53.1
32	Vytina	Arkadia	Peloponnese	37.67	22.19	2014	−7.2	−43.1

Table 1. Cont.

NO	Spring	Location	Region	North	East	Sampling Date	$\delta^{18}\text{O}$ (‰, VSMOW)	$\delta^2\text{H}$ (‰, VSMOW)
33	Vytina	Arkadia	Peloponnese	37.67	22.19	2015	−7.3	−45.2
34	Loutraki	Corinthia	Peloponnese	37.98	22.99	2014	−6.8	−47.9
35	Kaliani	Korinthia	Peloponnese	37.89	22.49	2014	−9.1	−61.4
36	Kaliani	Korinthia	Peloponnese	37.89	22.49	2015	−9.1	−56.9
37	Monastiraki Vounitsas	Aitolokarnanias	Stereia	38.84	20.96	2016	−7.5	−56.8
38	Helliniko	Attiki	Stereia	37.9	23.73	2018	−6.1	−34.9
39	Kalamos	Attiki	Stereia	38.14	23.74	2018	−7.7	−43.8
40	Kalamos	Attiki	Stereia	38.14	23.74	2018	−7.6	−42.8
41	Velouchi	Evrytania	Stereia	38.94	21.8	2015	−9.7	−66.5
42	Velouchi	Evrytania	Stereia	38.94	21.8	2018	−9.6	−65.9
43	Mornos	Fokida	Stereia	38.53	22.17	2015	−6.2	−37.1
44	Mornos	Fokida	Stereia	38.53	22.17	2018	−6.3	−38.5
45	Kamena Vourla	Fthiotida	Stereia	38.77	22.79	2014	−8.2	−48.8
46	kamena Vourla	Fthiotida	Stereia	38.77	22.79	2015	−5.0	−33.0
47	kamena Vourla	Fthiotida	Stereia	38.77	22.79	2018	−5.1	−30.8
48	Monastery	Fthiotida	Stereia	38.78	22.75	2015	−7.8	−51.0
49	Aliartos	Viotia	Stereia	38.37	23.1	2015	−7.9	−49.9
50	Kanalina	Karditsa	Thessaly	39.4	21.81	2018	−8.3	−52.4
51	Neo Monastiri	Karditsa	Thessaly	39.26	22.26	2018	−8.2	−54.0
52	Zografina	Karditsa	Thessaly	39.43	21.73	2018	−7.7	−46.8
53	Apostoli	Trikala	Thessaly	39.57	21.73	2018	−8.0	−48.9
54	Kotroni	Trikala	Thessaly	39.46	21.56	2018	−8.3	−51.9
55	Pyli	Trikala	Thessaly	39.47	21.62	2018	−7.8	−50.1
56	Agitis	Drama	Thraki	41.22	23.89	2014	−8.6	−57.0
57	Avas	Evros	Thraki	40.97	25.9	2014	−6.9	42.1
58	Doriskos	Evros	Thraki	40.86	26.13	2014	−6.3	−40.8
59	kounia	Evros	Thraki	41.28	25.9	2015	−7.9	−50.9
60	kounia	Evros	Thraki	41.28	25.9	2018	−7.8	−49.6
61	Pentalofos	Evros	Thraki	41.64	26.18	2015	−9.1	−61.4
62	Pentalofos	Evros	Thraki	41.64	26.18	2016	−8.8	−61.1
63	Plati	Evros	Thraki	41.58	26.32	2015	−7.8	−53.0
64	Plati	Evros	Thraki	41.58	26.32	2018	−7.9	−53.9
65	Polia	Evros	Thraki	41.43	26.22	2015	−6.1	−40.1
66	Polia	Evros	Thraki	41.43	26.22	2018	−6.2	−41.0
67	Rizia	Evros	Thraki	41.63	26.37	2016	−8.1	−55.0
68	Valtos	Evros	Thraki	41.55	26.31	2014	−8.6	−58.9
69	Elatia	Komotini	Thraki	41.5	24.35	2015	−8.1	−53.0
70	Elatia	Komotini	Thraki	41.5	24.35	2018	−8.0	−51.3
71	Nea Kessani	Rodopi	Thraki	41.13	25.08	2015	−7.2	−42.9
72	Nea Kessani	Rodopi	Thraki	41.13	25.08	2018	−6.1	−38.1
73	Agkistro	Serres	Thraki	41.38	23.73	2015	−8.5	−55.8
74	Ochiro	Serres	Thraki	41.21	23.89	2016	−8.7	−56.1

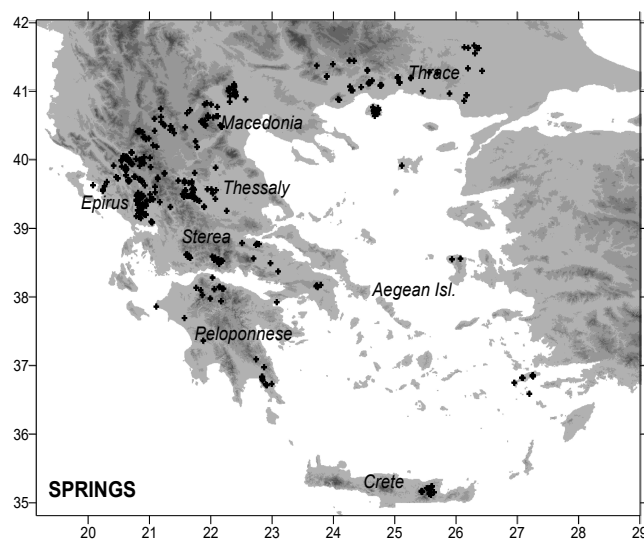


Figure 1. Geographical distribution of the stations considered in this work.

The area of Greece was divided in eight regions according to geographical criteria. Figure 2 presents the average $\delta^{18}\text{O}$, $\delta^2\text{H}$, deuterium excess (d), and Cl^- values for each region and for Greece.

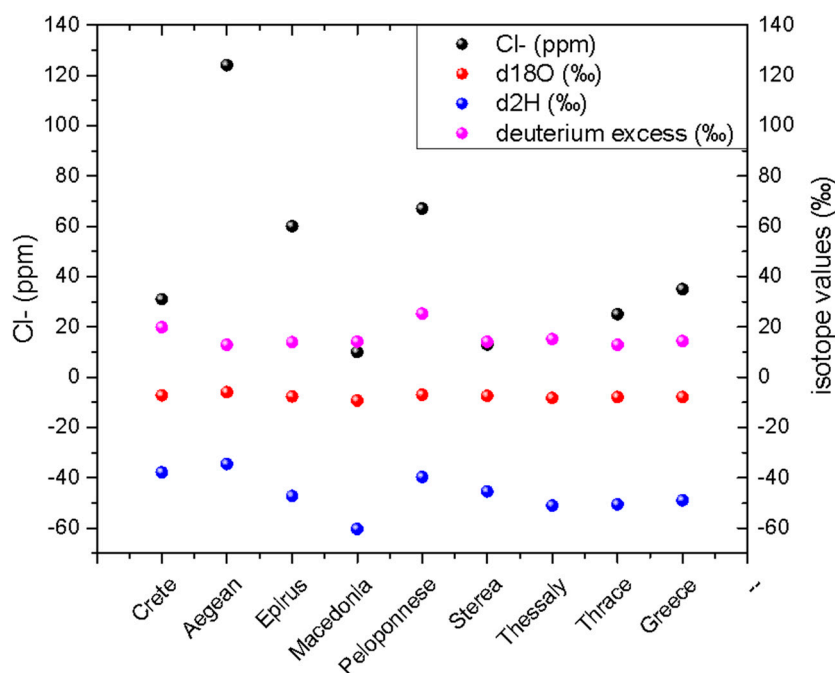


Figure 2. Average $\delta^{18}\text{O}$, $\delta^2\text{H}$, deuterium excess (d), and Cl^- values for each region and for Greece.

On the basis of that division and using the obtained average isotopic values (annual or other), local spring water lines (LWSLs) for spring water were calculated for each region, using the ordinary least squares regression (OLSR) and the generalized least squares (GENLS) that is suitable for cases where the errors of both x- and y-values are not constant and can also incorporate analytical or other Type B uncertainties [43]. In the cases where the analytical uncertainty was not reported, typical values of 0.1‰ for $\delta^{18}\text{O}$ and 1.0‰ for $\delta^2\text{H}$ were assumed. Statistical uncertainties were calculated as standard errors of the mean, or weighted mean, where applicable. We have constructed gridded isotopic data sets with a resolution of $30'' \times 30''$ (approximately 1 km \times 1 km) using the methodology proposed by Bowen [44] as implemented in Lykoudis [45]. The GTOPO30 data set maintained by the United States Geological Survey [46] was used. This methodology and its assessment are described elsewhere [40].

3. Regional Climate

The climate of Greece can be generally described as Mediterranean, with dry and hot summers and wet mild winter. Yet, the presence of the high altitude Pindos ridge that crosses mainland Greece creates a large variety of climatic conditions. Areas with a continental climate and cold winters exist, while a northward temperature gradient, from subtropical (south Greece) through temperate to cold (north Greece), is observed. Annual average temperatures range from 19.7 °C in Ierapetra (35.0° N), 17.7 °C in Athens (38.0° N), to 15.7 °C in Thessaloniki (40.5° N). Altitude and distance from the sea are also significant factors, with Karpenisi (38.9° N, 998 m) having a mean annual temperature of 11.7 °C in contrast to 17.6 °C recorded in Mytilene in the eastern Aegean (39.1 °C, 5 m). At elevations higher than 1500 m, snow represents a significant part of precipitations for a large part of the year. In southern and central Greece precipitation is unevenly distributed throughout the year, about 70–80% being measured between October and April. Further north, there is a second maximum during spring, whereas in the north-eastern mountains of Rodopi, precipitation has a somehow uniform distribution. Summer is the driest period for the entire area of Greece.

4. Results and Discussion

4.1. Spring Water

In Figure 3, we present the correlation between $\delta^{18}\text{O}$ and $\delta^2\text{H}$ in spring water. In the same figure, we present the global meteoric water line (GMWL) [47] the local meteoric water line (LMWL) for comparison [40]. The calculated relationship between $\delta^2\text{H}$ and $\delta^{18}\text{O}$ for spring waters has a slope of 7.3. Generally, an isotope relationship between $\delta^2\text{H}$ and $\delta^{18}\text{O}$ with a slope of <8 shows that the spring waters are subjected to evaporation relative to input. For the Crete and the Aegean islands, the oxygen isotope values of spring waters range between -7.90‰ and -4.30‰ , while for continental Greece it ranges between -10.90‰ and -3.193‰ . The deuterium values range between -46.3‰ and -26.6‰ , and -73.6‰ and -28.5‰ , for the same areas. The northern areas of Greece (Macedonia and Thrace) present the most negative values, while in the south part of Greece (Peloponnese) along with the Aegean islands, we observe the most positive values.

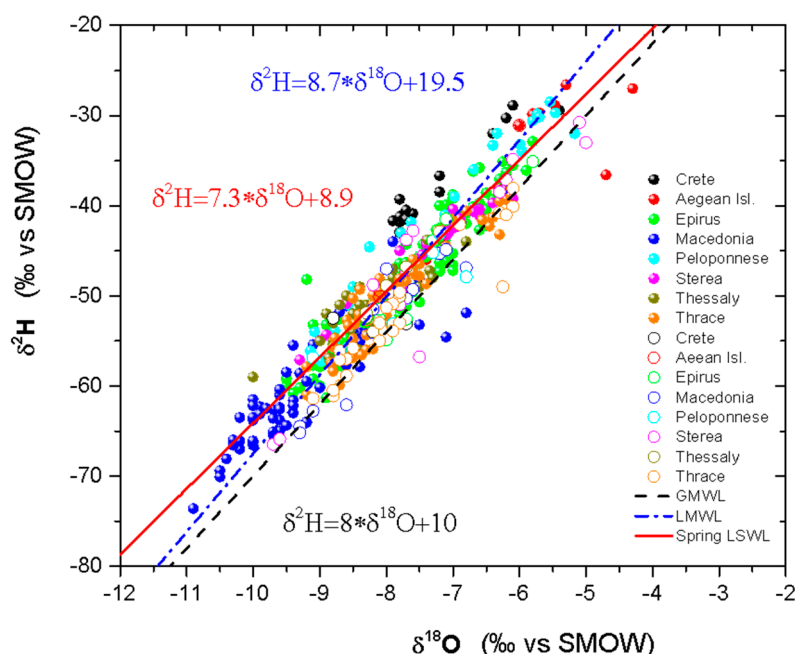


Figure 3. $\delta^{18}\text{O}$ versus $\delta^2\text{H}$ spring waters from bibliography data from the Greece territory. The hollow circles are unpublished data from this work. The black dash line is the global meteoric water line (GMWL), the blue dot-dash line is the local meteoric water line (LMWL), and the solid red line is a linear fit of the spring water data.

In Figure 4, we present the spring samples collected in the various regions of Greece and calculated the respective LSWL. Spring waters are more enriched in heavy isotopes in respect to meteoric water [40]. In general, in evaporative conditions, an enrichment of heavy isotopes in spring water is observed with a decrease in the deuterium excess value. In fact, in all regions' spring water, a decrease in the LSWL slope and intercept is observed in relation to the meteoric water, indicating that the spring water is affected by the influence of evaporation processes [47–49]. A possible cause for this enrichment is the partial evaporation of water before infiltration, the infiltration of recycled irrigation water, and evaporation of soil water. In northern Greece and Epirus, where there is a significant plant-covered area, the water is also alleviated of plant transpiration, probably changing the isotopic composition of the water. Moreover, an enrichment of the springs in Epirus is observed in relation to the spring waters from Thessaly. Presumably, the springs of Thessaly reflect the climatic conditions of central Greece. Because of the presence of Pindos ridge between Epirus and Thessaly, the clouds are discharged over Epirus and as a result only 'light' precipitation reaches Thessaly. More pronounced

evaporation due to more arid conditions through Greece, from north to south, is not clearly observed; however, it seems that the evaporated spring waters are more commonly located in Crete and in eastern Aegean rather than in Thrace, Macedonia, and Epirus.

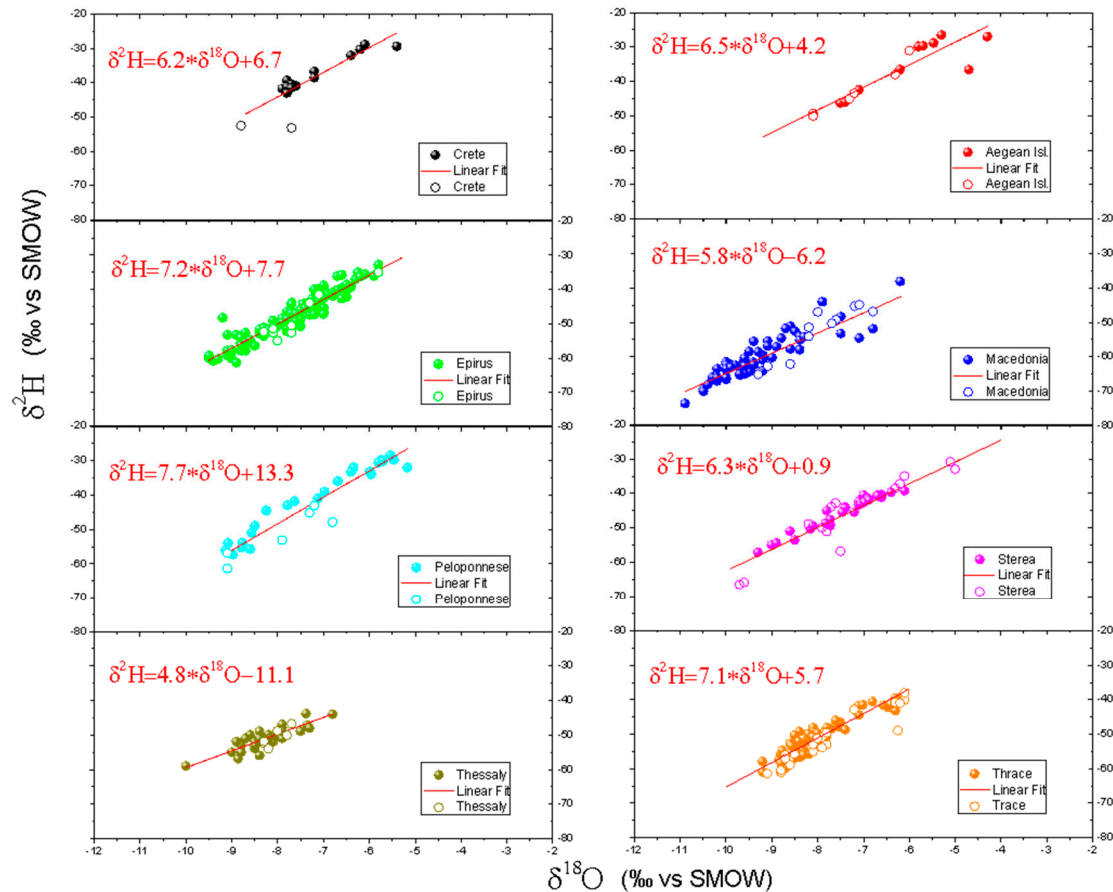


Figure 4. Local spring water lines (LSWLs) of various regions of Greece. The solid circles are bibliography data, while the hollow circles are unpublished data from this work.

4.2. Geographical Distribution of $\delta^{18}\text{O}$ Values in Precipitation and Spring Water

The geographical distribution of spring water composed of $\delta^{18}\text{O}$ – $\delta^2\text{H}$ is shown in Figure 5a,b. The regression models obtained are:

$$\delta^{18}\text{O}_{\text{spring}} = -27 + 1.4 \cdot \text{Latitude} - 0.02 \cdot \text{Latitude}^2 - 0.00148 \cdot \text{Altitude}, R^2 = 0.55$$

As a general feature, a gradual rise of values of spring water $\delta^{18}\text{O}$ – $\delta^2\text{H}$ across Greece can be observed, proceeding from higher altitudes towards the coastal areas. In addition, a gradual rise of values of $\delta^{18}\text{O}$ – $\delta^2\text{H}$ is observed in relation to the locations of the stations relative to the sea.

In northern Greece, the values of $\delta^{18}\text{O}$ and $\delta^2\text{H}$ of the spring water vary from -7.5‰ to -45‰ for the plains, to lower than -8‰ and -55‰ for massif areas, and from -6.5‰ to -5.5‰ and -35‰ for coastal lowlands. From west to east, apart from Peloponnese, more positive spring water values are observed at the western coast, while the most negative values are reported in the central part of the mainland where the mountain ranges are located. Plains with medium isotopic values extend between coasts and the mainland massifs. In Peloponnese, the values for massif areas still have the most negative $\delta^{18}\text{O}$ values, close to -9.5‰ , and -55‰ for $\delta^2\text{H}$, but the coastal areas present uniformly enriched values, close to -5‰ and -25‰ for $\delta^{18}\text{O}$ and $\delta^2\text{H}$, respectively, regardless of their western or

eastern location. The same is true for the islands of the southern Aegean and coastal areas comprising the largest part of Crete.

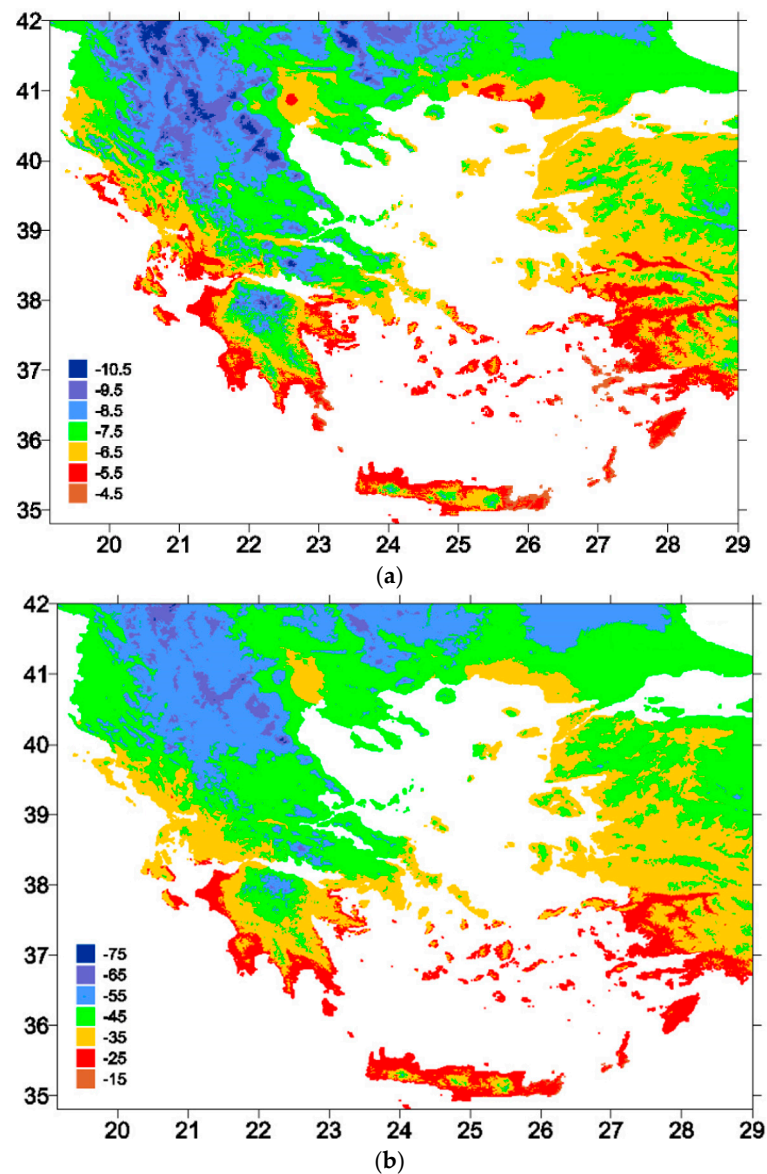


Figure 5. (a) The geographical distribution of spring water $\delta^{18}\text{O}$; (b) the geographical distribution of spring water $\delta^2\text{H}$.

The factors that can be identified as influential in these spring data are the location of the stations relative to the sea and the altitude effect. A general feature of the spatial distribution for spring water $\delta^{18}\text{O}$ is also a gradual rise of values when proceeding from higher altitudes towards the coastal areas. The mountainous regions of Greece are characterized by $\delta^{18}\text{O}$ and $\delta^2\text{H}$ values ranging from -10.5‰ to -8.5‰ and -75‰ to -55‰ , respectively, whereas the lowlands of northern Greece, extending from Thessaloniki to Evros, present more positive values, ranging from -7.5‰ to -5.5‰ and -45‰ to -35 , respectively. These differences in the isotopic values between the mountain regions and the northern lowlands are an indication of the different isotopic composition of the recharging rainfalls. Possible explanations, like different hydrological circuits, are excluded since all the springs considered in this study have low a Cl^- content. In addition, this isotopic enrichment effect may indicate a contribution from vapor originating from evaporation of the seawater surface [50]. Such a scenario is

facilitated by the low elevation of the river valleys of northern Greece, these include the deltas of the biggest rivers of the country (from east to west: Evros, Nestos, Strymonas, Axios, and Aliakmonas). Therefore, in the southern part of northern Greece, extending from Thessaloniki to Evros, the enriched isotopic values are mainly the result of the addition of water vapor from the Aegean Sea.

Comparing the western mainland in relation to the eastern part of Greece, we observe the most negative values in the eastern part, as expected because of the orographic lifting effect of the Pindos ridge that separates Greece into two parts; the western with rich rainfalls and the eastern with the most depleted ones. Contrary to the above, an isotopic anomaly is noticed in the area of the Sperchios delta and the Attica peninsula. The -6.5‰ and -35‰ value of $\delta^{18}\text{O}$ and $\delta^2\text{H}$, respectively, that is observed in the Sperchios plain, at a point more than half way between the east and west coast undoubtedly indicates that this area is affected by water vapor transported from the Aegean Sea.

The highest spring water values of $\delta^{18}\text{O}$ and $\delta^2\text{H}$ for all continental Greece, higher than -5.5‰ and -25‰ , respectively, are reported at the western and eastern part of Peloponnese. This pattern might be seen as indicating a climatic transition towards warmer and drier climatic conditions from the Greek mainland to Peloponnese, a fact related to increased evaporation processes.

Figure 6 presents a map of the differences between the gridded $\delta^{18}\text{O}$ data for springs and precipitation. We observe an enrichment of spring waters by about $1\text{--}2\text{‰}$ compared to the precipitation for the western part of Greece, and more general at the western side of massifs and in NE Greece, indicating a significant contribution from melting snow. For springs located in the plains of Thessaly and Macedonia, as well as Peloponnese and Crete, we observe very similar $\delta^{18}\text{O}$ values as the local precipitation with the exception of certain springs that appear depleted in relation to precipitation indicating recharging by precipitation occurring at significantly higher altitudes [51].

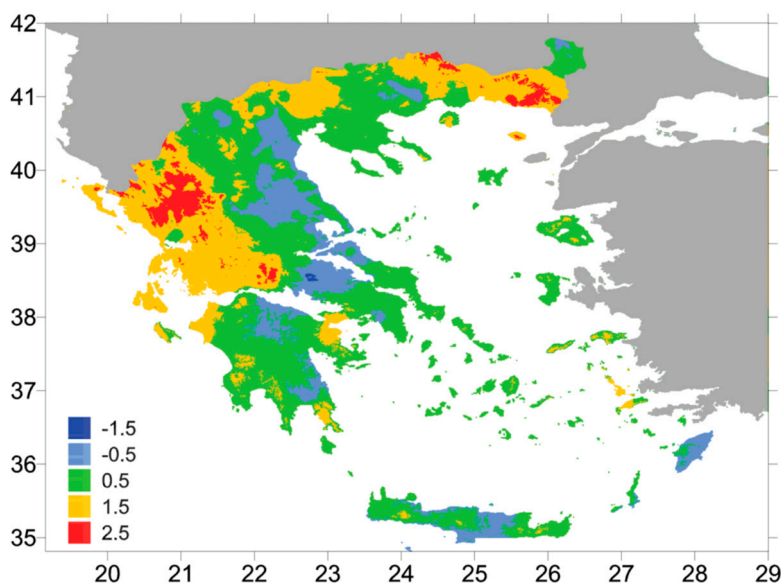


Figure 6. Map of the differences between the gridded $\delta^{18}\text{O}$ data for springs and precipitation.

4.3. $\delta^{18}\text{O}$ Values in Relation to the Salinity of Spring Water

The samples collected from springs all over Greece, with high Cl contents, represent cold waters. The regions from which the samples were collected cover a wide area of Greece. Many samples come from islands (Aegean Isl., Crete, and Chios) and from continental Greece (Sterea area: Asopos, Axios, Kalamos; Peloponnese: Ilia, and Sparta). The quality of these waters has been degraded by the elevated salinity.

According to Figure 7a,b which presents the variation of Cl^- versus $\delta^{18}\text{O}$ and $\delta^2\text{H}$, all the water samples are on an ideal mixing line between seawater and fresh water. This suggests that

the observed Cl^- contents derive predominantly from seawater, which is more or less diluted by fresh water and that the supply of these ions by rock leaching is negligible. The locations of the data points also indicate that the samples are distributed along different lines, between seawater and fresh water of meteoric origin, corresponding to different sampling zones. If these lines were mixing lines, their x -axis intercepts would represent the $\delta^{18}\text{O}$ and $\delta^2\text{H}$ contents of the meteoric component of the mixtures. This corresponds to values between -9.3‰ and -6.2‰ , and -58.9 and -32.3 for $\delta^{18}\text{O}$ and $\delta^2\text{H}$, respectively.

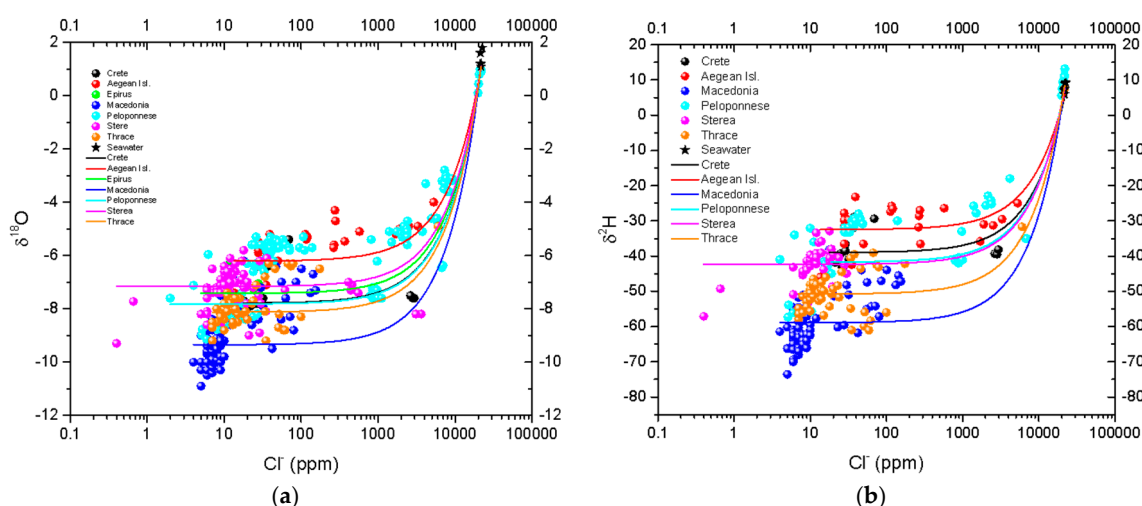


Figure 7. (a,b) Variation of Cl^- versus $\delta^{18}\text{O}$ and $\delta^2\text{H}$, respectively. Seawater-precipitation lines for each region are provided.

A lot of samples plot relatively close to the seawater–groundwater mixing line as observed in Figure 7, and at the same time contain more than 2500 ppm of Cl^- . This indicates that the seawater intrusion is more than 10%. On the basis of the stable isotope– Cl^- relations, balance equations can be used to determine the marine contribution for these samples. The same type of balance equation [17] can also be made using only Cl^- contents, with the assumption that Cl^- is provided only by the marine component. These balances give very similar results: <50% marine contribution to the water of Sparta, <25% marine contribution to the water of Ilia, <20% marine contribution to the water of Axios and Chios, and <15% marine contribution to the water of Crete and Asopos.

5. Conclusions

The isotopic compositions of spring waters across Greece result from various processes, including the contribution of moisture sources and the Pindos ridge.

The first map of the isotopic composition of water springs over Greece is presented. From this map we can conclude a depletion of $\delta^{18}\text{O}$ in spring water at higher altitudes (altitude effect), and a gradual rise of values of $\delta^{18}\text{O}$ in relation to the location of the stations relative to the sea. Furthermore, we observe a large area with relatively depleted values in the eastern part of Greece that is related to the lower altitudes of the region and indicates a possible orographic shadow effect (Pindos ridge). The highest $\delta^{18}\text{O}$ values in spring water are reported in south Greece (Peloponnese and Crete), indicating a hot and dry climate and a possible climatic transition towards warmer and drier conditions that could explain the supposed evaporation increase.

Author Contributions: D.E., D.G. and P.D. performed stable isotope measurements and analysis, L.S. performed the isoscape map analysis and K.E. provided samples and worked on the revision of the manuscript. The composition of the original manuscript was performed by D.E., P.D. and L.S.

Funding: Partial funding by the Humanitarian and Human Rights Resource Center of the American Academy of Forensic Sciences.

Conflicts of Interest: The authors declare no conflict of interest.

References

1. Gat, J.; Carmi, I. Evolution of the isotopic composition of atmospheric waters in the Mediterranean Sea area. *J. Geophys. Res.* **1970**, *75*, 3039–3048. [[CrossRef](#)]
2. Gat, J.; Klein, B.; Kushnir, Y.; Roether, W.; Wernli, H.; Yam, R.; Shemesh, A. Isotope composition of air moisture over the Mediterranean Sea: An index of the air–sea interaction pattern. *Tellus B* **2003**, *55*, 953–965. [[CrossRef](#)]
3. Ambrose, S.H. Isotopic analysis of palaeodiets: Methodological and interpretive consideration. In *Investigations of Ancient Human Tissue*; Gordon & Breach Science Publishers: Langhorne, PA, USA, 1993; Volume 10, pp. 59–130.
4. Garnsey, P. *Food and Society in Classical Antiquity*; Cambridge University Press: Cambridge, UK, 1999; ISBN 0521645883.
5. Ambrose, S.H.; Norr, L. Experimental evidence for the relationship of the carbon isotope ratios of whole diet and dietary protein to those of bone collagen and carbonate. In *Prehistoric Human Bone*; Springer: New York, NY, USA, 1993; pp. 1–37.
6. Bartelink, E.J.; Berg, G.E.; Beasley, M.M.; Chesson, L.A. Application of stable isotope forensics for predicting region of origin of human remains from past wars and conflicts. *Ann. Anthropol. Pract.* **2014**, *38*, 124–136. [[CrossRef](#)]
7. Bartelink, E.; Berry, R.; Chesson, L. Stable isotopes and human provenancing. In *Advances in Forensic Human Identification*; CRC Press: Boca Raton, FL, USA, 2014; pp. 165–192.
8. Ehleringer, J.R.; Bowen, G.J.; Chesson, L.A.; West, A.G.; Podlesak, D.W.; Cerling, T.E. Hydrogen and oxygen isotope ratios in human hair are related to geography. *Proc. Natl. Acad. Sci. USA* **2008**, *105*, 2788–2793. [[CrossRef](#)] [[PubMed](#)]
9. Ehleringer, J.R.; Thompson, A.H.; Podlesak, D.W.; Bowen, G.J.; Chesson, L.A.; Cerling, T.E.; Park, T.; Dostie, P.; Schwarcz, H. A framework for the incorporation of isotopes and isoscapes in geospatial forensic investigations. In *Isoscapes*; Springer: New York, NY, USA, 2010; pp. 357–387.
10. Bencini, A.; Duchi, V.; Casatello, A.; Kolios, N.; Fytikas, M.; Sbaragli, L. Geochemical study of fluids on Lesbos island, Greece. *Geothermics* **2004**, *33*, 637–654. [[CrossRef](#)]
11. Christodoulou, T.; Leontiadis, I.; Morfis, A.; Payne, B.; Tzimourtas, S. Isotope hydrology study of the Axios River plain in northern Greece. *J. Hydrol.* **1993**, *146*, 391–404. [[CrossRef](#)]
12. Dimitriou, E.; Zacharias, I. Using state-of-the-art techniques to develop water management scenarios in a lake catchment. *Hydrol. Res.* **2007**, *38*, 79–97. [[CrossRef](#)]
13. Dotsika, E. Utilisation du Geothermometre Isotopique Sulfate-Eau en Milieux de Haute Temperature Sous Influence Marine Potentielle: Les Systemes Geothermaux de Grece. Ph.D. Thesis, University Paris-Sud, Orsay, France, 1991.
14. Dotsika, E.; Michelot, J.-L. Origine et températures en profondeur des eaux thermales d'Ikaria (Grèce). *C. R. Acad. Sci.* **1992**, *315*, 1261–1266.
15. Dotsika, E.; Poutoukis, D.; Michelot, J.; Kloppmann, W. Stable isotope and chloride, boron study for tracing sources of boron contamination in groundwater: Boron contents in fresh and thermal water in different areas in Greece. *Water Air Soil Pollut.* **2006**, *174*, 19–32. [[CrossRef](#)]
16. Dotsika, E.; Leontiadis, I.; Poutoukis, D.; Cioni, R.; Raco, B. Fluid geochemistry of the Chios geothermal area, Chios Island, Greece. *J. Volcanol. Geotherm. Res.* **2006**, *154*, 237–250. [[CrossRef](#)]
17. Dotsika, E.; Poutoukis, D.; Michelot, J.; Raco, B. Natural tracers for identifying the origin of the thermal fluids emerging along the Aegean Volcanic arc (Greece): Evidence of Arc-Type Magmatic Water (ATMW) participation. *J. Volcanol. Geotherm. Res.* **2009**, *179*, 19–32. [[CrossRef](#)]
18. Duriez, A.; Marlin, C.; Dotsika, E.; Massault, M.; Noret, A.; Morel, J. Geochemical evidence of seawater intrusion into a coastal geothermal field of central Greece: Example of the Thermopylae system. *Environ. Geol.* **2008**, *54*, 551–564. [[CrossRef](#)]

19. Grassi, S.; Kolios, N.; Mussi, M.; Saradeas, A. Groundwater circulation in the Nea Kessani low-temperature geothermal field (NE Greece). *Geothermics* **1996**, *25*, 231–247. [\[CrossRef\]](#)
20. Griffiths, S.J.; Street-Perrott, F.A.; Holmes, J.A.; Leng, M.J.; Tzedakis, C. Chemical and isotopic composition of modern water bodies in the Lake Kopais Basin, central Greece: Analogues for the interpretation of the lacustrine sedimentary sequence. *Sediment. Geol.* **2002**, *148*, 79–103. [\[CrossRef\]](#)
21. Kallergis, G.; Leontiadis, I. Isotope hydrology study of the Kalamos Attikis and Assopos riverplain areas in Greece. *J. Hydrol.* **1983**, *60*, 209–225. [\[CrossRef\]](#)
22. Kavouridis, T.; Kuris, D.; Leonis, C.; Liberopoulou, V.; Leontiadis, J.; Panichi, C.; La Ruffa, G.; Caprai, A. Isotope and chemical studies for a geothermal assessment of the island of Nisyros (Greece). *Geothermics* **1999**, *28*, 219–239. [\[CrossRef\]](#)
23. Kelepertsis, A.; Alexakis, D.; Kita, I. Environmental geochemistry of soils and waters of Susaki area, Korinthos, Greece. *Environ. Geochem. Health* **2001**, *23*, 117–135. [\[CrossRef\]](#)
24. La Ruffa, G.; Panichi, C.; Kavouridis, T.; Liberopoulou, V.; Leontiadis, J.; Caprai, A. Isotope and chemical assessment of geothermal potential of Kos Island, Greece. *Geothermics* **1999**, *28*, 205–217. [\[CrossRef\]](#)
25. Leontiadis, J. *Isotope Hydrology Study of Molai Area in Laconia*; Internal Report, Demo 81/4; Democritos Nuclear Research Center: Athens, Greece, 1981.
26. Leontiadis, I.; Payne, B.; Letsios, A.; Papagianni, N.; Kakarelis, D.; Chadjiagorakis, D. Isotope hydrology study of Kato Nevrokopi of Drama. In Proceedings of the Symposium on Isotope Hydrology, Vienna, Austria, 12–16 September 1983; pp. 193–206.
27. Leontiadis, I.; Payne, B.; Christodoulou, T. Isotope hydrology of the Aghios Nikolaos area of Crete, Greece. *J. Hydrol.* **1988**, *98*, 121–132. [\[CrossRef\]](#)
28. Leontiadis, I.; Stamos, A.; Manakos, A. Isotope hydrology study of the wider area of Kozani, Greece. In Proceedings of the 6th International Symposium on Water Tracing, Karlsruhe, Germany, 21–26 September 1992; pp. 233–240.
29. Leontiadis, I.; Vergis, S.; Christodoulou, T. Isotope hydrology study of areas in Eastern Macedonia and Thrace, Northern Greece. *J. Hydrol.* **1996**, *182*, 1–17. [\[CrossRef\]](#)
30. Leontiadis, I.; Nikolaou, E. Environmental isotopes in determining groundwater flow systems, northern part of Epirus, Greece. *Hydrogeol. J.* **1999**, *7*, 219–226. [\[CrossRef\]](#)
31. Leontiadis, I.; Nikolaou, E.; Dotsika, E. Environmental isotopes in determining groundwater flow systems, Epirus, Greece. *Bull. Geol. Soc. Greece* **2006**, *14*, 47–70.
32. Michelot, J.-L.; vet Dotsika, E.; Fytikas, M. A hydrochemical and isotopic study of thermal waters on Lesbos Island (Greece). *Geothermics* **1993**, *22*, 91–99. [\[CrossRef\]](#)
33. Mitropoulos, P.; Kita, I. Geochemistry of oxygen and hydrogen isotopes in Greek regional waters. In *Proceedings of the 4th Hydrogeological Congress*; Commission of Greece: Athens, Greece, 1997; pp. 285–291.
34. Payne, B.; Dimitroulas, D.; Leontiadis, I.; Kallergis, G.; Christodoulou, T. Environmental isotope data in the Western Thessaly valley, Greece: Use of mathematical model for quantitative evaluations with tritium. *Bull. Geol. Soc. Greece* **1976**, *12*, 29–94.
35. Stratikopoulos, K. Hydrogeological and Hydrochemical Study of Thermometallic Springs of Western Peloponnese Using Stable Isotopes. Ph.D. Thesis, University of Patras, Patras, Greece, 2007.
36. Kolios, N. Low Enthalpy Geochemical Study—The Geothermal Field of Nea Kessani. Ph.D. Thesis, University of Athens, Athens, Greece, 1993.
37. Leontiadis, E.D.; Romaidis, I. Isotope hydrology study of the wider area of Orestias. In Proceedings of the 5th Panhellenic Hydrogeological Symposium, Limasol, Cyprus, 1999; pp. 463–479, (In Greek with English Abstract).
38. Leontiadis, A.S. Isotope hydrology study of the upper flow of Aliakmon river. In Proceedings of the 5th Panhellenic Hydrogeological Symposium, Limasol, Cyprus, 1999; pp. 481–496, (In Greek with English Abstract).
39. Leontiadis, C.S. Isotope hydrology study of the Louros Riverplain area, Epirus, Greece. In Proceedings of the 5th International Symposium on Underground Water Tracing, Athens, Greece, 22–27 September 1986; pp. 75–90.
40. Dotsika, E.; Lykoudis, S.; Poutoukis, D. Spatial distribution of the isotopic composition of precipitation and spring water in Greece. *Glob. Planet. Chang.* **2010**, *71*, 141–149. [\[CrossRef\]](#)

41. Epstein, S.; Mayeda, T. Variation of ^{18}O content of water from natural sources. *Geochim. Cosmochim. Acta* **1953**, *4*, 213–224. [[CrossRef](#)]
42. Coleman, M.L.; Shepherd, T.J.; Durham, J.J.; Rouse, J.E.; Moore, G.R. Reduction of water with zinc for hydrogen isotope analysis. *Anal. Chem.* **1982**, *54*, 993–995. [[CrossRef](#)]
43. Argiriou, A.A.; Lykoudis, S. Isotopic composition of precipitation in Greece. *J. Hydrol.* **2006**, *327*, 486–495. [[CrossRef](#)]
44. Bowen, G.J.; Wilkinson, B. Spatial distribution of $\delta^{18}\text{O}$ in meteoric precipitation. *Geology* **2002**, *30*, 315–318. [[CrossRef](#)]
45. Lykoudis, S.P.; Argiriou, A.A. Gridded data set of the stable isotopic composition of precipitation over the eastern and central Mediterranean. *J. Geophys. Res. Atmos.* **2007**. [[CrossRef](#)]
46. GTOPO30 (Global 30 Arc-Second Elevation Data Set). USGS, Ed. Available online: <https://lta.cr.usgs.gov/GTOPO30> (accessed on 1 January 2015).
47. Craig, H. Isotopic variations in meteoric waters. *Science* **1961**, *133*, 1702–1703. [[CrossRef](#)] [[PubMed](#)]
48. Craig, H.; Gordon, L.; Horibe, Y. Isotopic exchange effects in the evaporation of water: 1. Low-temperature experimental results. *J. Geophys. Res.* **1963**, *68*, 5079–5087. [[CrossRef](#)]
49. Ehhalt, D.; Knott, K.; Nagel, J.; Vogel, J. Deuterium and oxygen 18 in rain water. *J. Geophys. Res.* **1963**, *68*, 3775–3780. [[CrossRef](#)]
50. Longinelli, A.; Anglesio, E.; Flora, O.; Iacumin, P.; Selmo, E. Isotopic composition of precipitation in Northern Italy: Reverse effect of anomalous climatic events. *J. Hydrol.* **2006**, *329*, 471–476. [[CrossRef](#)]
51. Rozanski, K.; Sonntag, C.; Münnich, K. Factors controlling stable isotope composition of European precipitation. *Tellus* **1982**, *34*, 142–150. [[CrossRef](#)]



© 2018 by the authors. Licensee MDPI, Basel, Switzerland. This article is an open access article distributed under the terms and conditions of the Creative Commons Attribution (CC BY) license (<http://creativecommons.org/licenses/by/4.0/>).